Implementations of the finite element method for the collective model of atomic nuclei

Gusev A.A. (JINR, Dubna, Russia)

in collaboration with:
Statement of the problem: Derbov V.L. (SSU, Saratov, Russia),
Deveikis A. (VMU, Kaunas, Lithuania) Hess P.O.(UNAM, Mexico, Mexico),
Mardyban E.V., Vinitsky S.I.(JINR, Dubna, Russia),
Implementations: Blinkov Yu.A. (SSU, Saratov, Russia),
Buša J. Jr., Chuluunbaatar G., Chuluunbaatar O. (JINR, Dubna, Russia)

Outline

- Introduction
- Formulation of BVP and GTM and FEM schemes
- BVP for five-dimensional quarupole Hamiltonian model
- Benchmark calculations of ^{154}Gd and ^{238}U in the RMF model
- Conclusions

October 24, 2024

Mathematical Modeling and Computational Physics, 2024, Yerevan, Armenia

Introduction: Recalling

Finite element methods (FEM)

• Kumar, K. and Baranger, M.: Complete numerical solution of Bohr's collective Hamiltonian, Nucl. Phys. A 92, 608–652 (1967).
• Troltenier, D., Maruhn, J. A., Greiner, W., and Hess, P. O.: A general numerical solution of collective quadrupole surface motion applied to microscopically calculated potential energy surfaces, Z. Phys. A – Hadrons and Nuclei 343, 25–34 (1992).
• Batgerel, B., Blinkov, Yu.A., Vinitsky, S.I., Gusev, A.A.,Chuluunbaatar, O.,Deveikis, A., Buša Jr.,J., Chuluunbaatar, G., and Ulziibayar, V.: Schemes of finite element method for solving multidimensional boundary value problems, J. Math. Sci., New York 279, 738 (2024)

Galerkin methods (GTM) single or double basis sets for single or double wells

• Hess, P.O., Seiwert, M., Maruhn, J., and Greiner, W.: General collective model and its application to $^{238}_{92}$U, Z. Phys. A – Atoms and Nuclei 296, 147-163 (1980)
• Troltenier, D., Maruhn, J. A., and Hess, P. O.: Numerical application of the geometric collective model, In: Langanke, K., Maruhn, J.A., Konin, S.E. (eds.) Computational Nuclear Physics 1, 105–128, Springer–Verlag, Berlin (1991)
• Libert, J., Girod, M., and Delaroche, J.-P. L.: Microscopic descriptions of superdeformed bands with the Gogny force: Configuration mixing calculations in the A∼190 mass region, Phys. Rev. C 60, 054301–1–26 (1999).
• Delaroche, J.-P., Girod, M., Gouttea, H., Libert, J.: Structure properties of even-even actinides at normal and super deformed shapes analysed using the Gogny force, Nucl. Phys. A 771, 103–168 (2006)
•J. Libert, J.-P. Delaroche, and M. Girod, Five-dimensional collective Hamiltonian with the Gogny force: An ongoing saga. Eur. Phys. J. A (2016) 52: 197

Formulation of BVP and GTM and FEM schemes

Self-adjoint BVP for the elliptic differential equation

$$(T+V(x)-E)\,\Phi(x)=0, \quad T=-\frac{1}{g_0(x)}\sum_{i,j=1}^{d}\frac{\partial}{\partial x_i}g_{ij}(x)\frac{\partial}{\partial x_j}, \quad x=(x_1,\ldots,x_d)\in\Omega\in\mathcal{R}^d, \tag{1}$$

$$g_0(x)>0, \quad g_{ji}(x)=g_{ij}(x), \quad + \text{ Neumann or Dirichlet boundary conditions.} \tag{2}$$

The expansion over the appropriate basis functions $N_l(x)$

in the Galerkin type method (GTM), or finite element method (FEM)

$$\Phi_m^h(x)=\sum_{l=1}^{L_\Omega}N_l(x)\Phi_{lm}^h. \tag{3}$$

Algebraic generalized eigenvalue problem

$$(\mathbf{A}-\mathbf{B}E_m^h)\Phi_m^h=0, \quad (\Phi_m^h)^T\mathbf{B}\Phi_m^h=1, \tag{4}$$

with respect to E_m^h and Φ_m^h.

In the FEM, the polyhedral domain $\bar{\Omega}$ is divided into subdomains Δ_q, called finite elements $\bar{\Omega} = \bar{\Omega}_h(x) = \bigcup_{q=1}^{Q} \Delta_q, \quad \bar{\Omega} \subset \mathcal{R}^d$.

The local basis functions , LIPs or HIPs are introduced: $\hat{\varphi}_{rq}^{\kappa}(x), \quad x \in \Delta_q$.

The piecewise polynomial functions (PPFs) constructed by joining the polynomials $\hat{\varphi}_{rq}^{\kappa p'}(x)$ on the finite elements $\Delta_q \in \bar{\Omega}_h(x)$

$$N_l(x) = \bigcup_{q=1}^{Q} \{\hat{\varphi}_{rq}^{\kappa}(x) | x \in \Delta_q\}. \qquad (5)$$

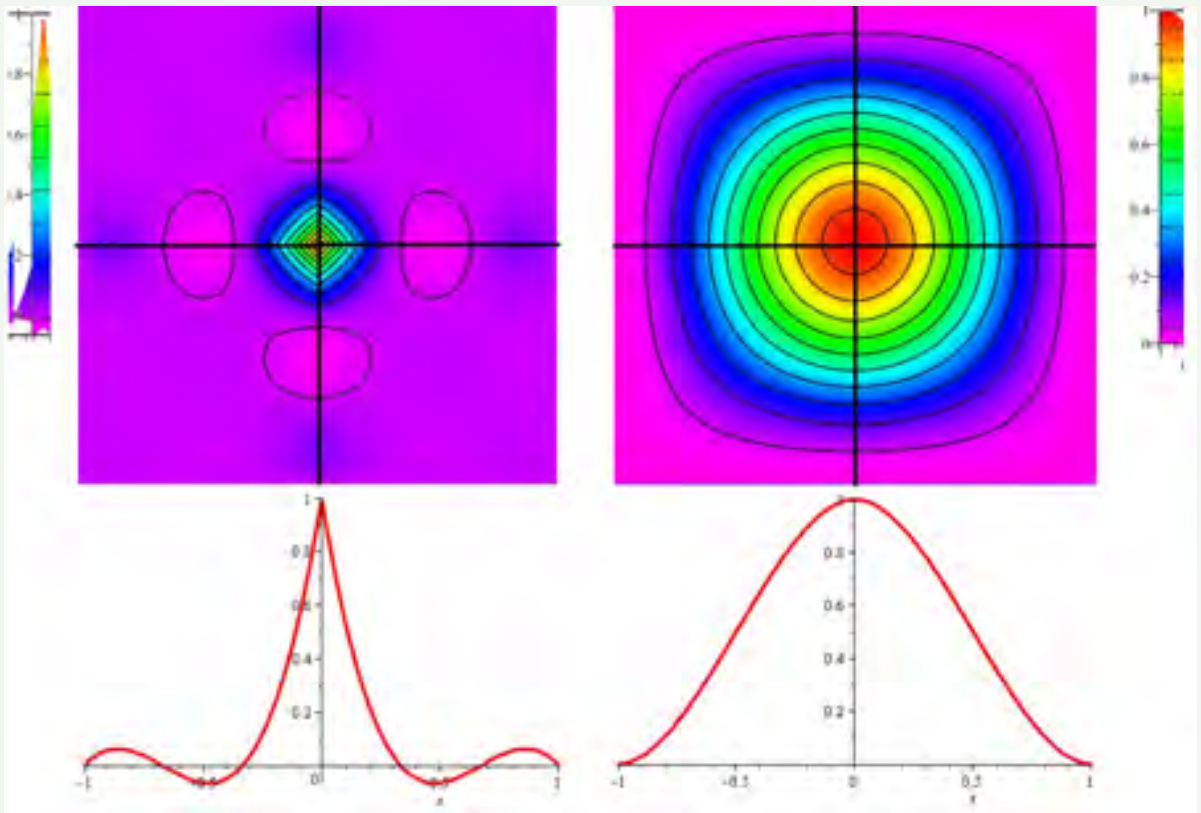

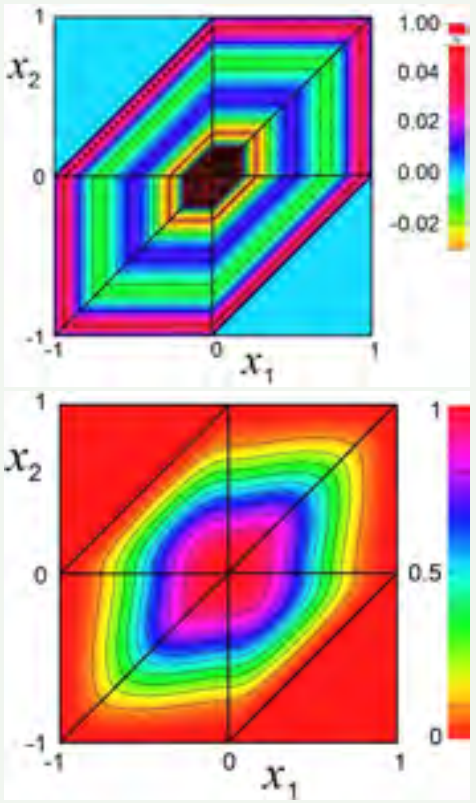

Structures of mass and stiffness matrices A and B

2D

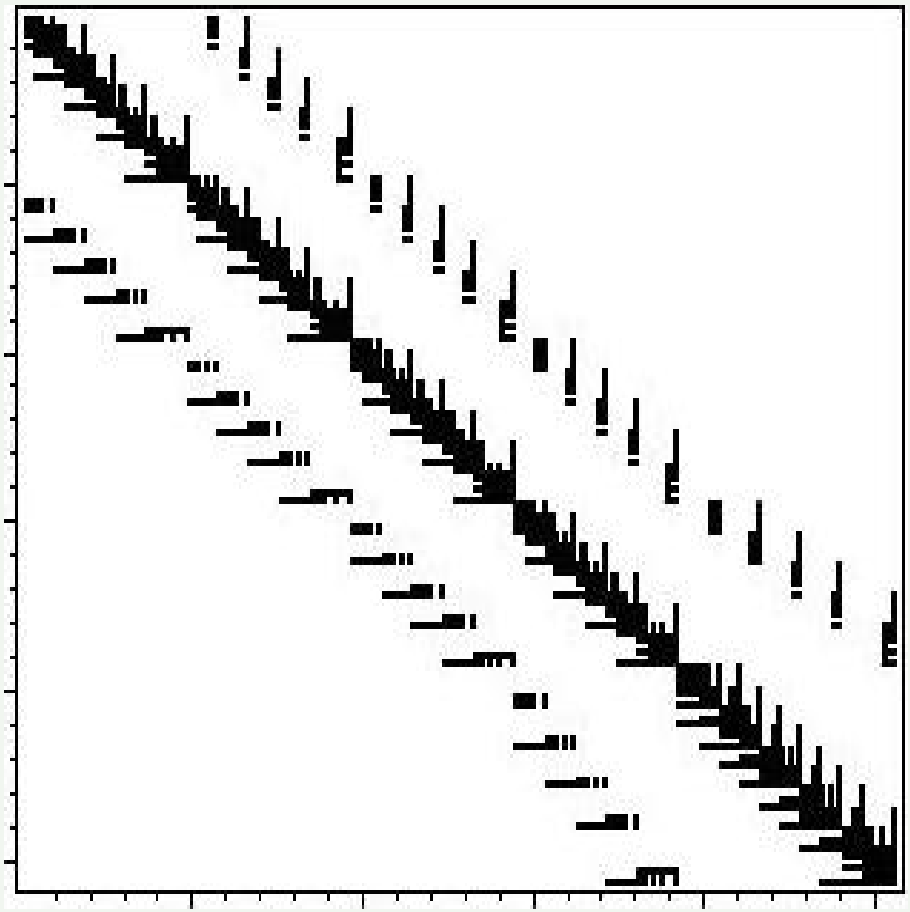

3D

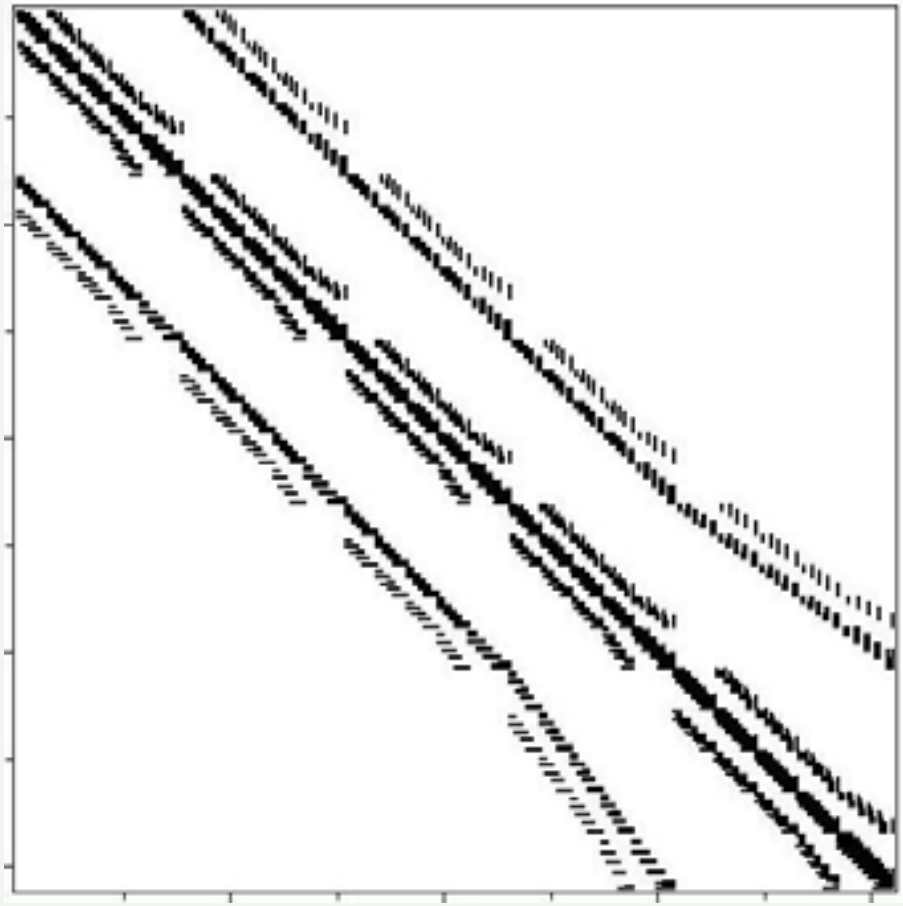

5DBVP for the five-dimensional quarupole Hamiltonian(5DQH)

The Schrödinger equation with respect to eigenfunction $\Psi_{nIM} \equiv \Psi_{nIM}(\beta, \gamma, \vartheta_i)$ and the corresponding eigenvalues of energy E_{nI} has the form

$$\frac{2}{\hbar^2}(\hat{H} - E_{nI})\Psi_{nIM} = \left(\hat{T}_{\text{vib}} + \hat{T}_{\text{rot}} + \frac{2}{\hbar^2}(V - E_{nI})\right)\Psi_{nIM} = 0. \tag{6}$$

orthogonality and normalization conditions

$$\int_{\Omega_5} \Psi_{nIM}\Psi_{n'I'M'} g_0(\beta, \gamma) d\beta d\gamma \sin\vartheta_2 d\vartheta_1 d\vartheta_2 d\vartheta_3 = \delta_{nn'}\delta_{II'}\delta_{MM'}. \tag{7}$$

The eigenfunction Ψ_{nIM} in the representation of the angular momentum I and its projections K and M on the third axes of the intrinsic and laboratory frames

$$\Psi_{nIM}(\beta, \gamma, \vartheta_i) = \sum_{K \geq 0, even}^{I} \mathcal{D}^{I*}_{MK}(\vartheta_i)\Phi_{nIK}(\beta, \gamma), \tag{8}$$

where $\mathcal{D}^{I*}_{MK}(\vartheta_i)$ are the normalized D-functions with the space parity $\hat{\pi} = \pm 1$

$$\mathcal{D}^{I*}_{MK}(\vartheta_i) = \sqrt{\frac{2I+1}{8\pi^2}} \frac{(D^{I*}_{MK}(\vartheta_i) + \hat{\pi}(-1)^I D^{I*}_{M-K}(\vartheta_i))}{\sqrt{2(1+\delta_{K0})}}. \tag{9}$$

2DBVP for five-dimensional quarupole Hamiltonian(5DQH)

The unknown set of $I_{\max}$ internal components $\Phi_{nIK} \equiv \Phi_{nIK}(\beta,\gamma)$, where $K = 0, 2, \ldots, I$ for even I, or $K = 2, 4, \ldots, (I-1)$ for odd I, compose the vector eigenfunction Φ_{nI} corresponding to the eigenvalue E_n^I (in MeV) of the BVP for a system of $I/2+1$ or $(I-1)/2$ equations for even or odd I, respectively:

$$\left[\hat{T}_{\rm vib} + T^I_{KK} + \frac{2}{\hbar^2}(V - E_{nI})\right]\Phi_{nIK} + T^I_{KK+2}\Phi_{nIK+2} + T^I_{KK-2}\Phi_{nIK-2} = 0,$$

$$\hat{T}_{\rm vib}(x_1,x_2) = -\frac{1}{g_0(x_1,x_2)}\sum_{i,j=1}^{2}\frac{\partial}{\partial x_i}g_{ij}(x_1,x_2)\frac{\partial}{\partial x_j},$$

$$T^I_{KK} = (I(I+1) - K^2)\left(\frac{1}{2J_1} + \frac{1}{2J_2}\right) + \frac{K^2}{J_3},\ T^I_{KK\pm2} = \left(\frac{1}{4J_1} - \frac{1}{4J_2}\right)C^I_{KK\pm2},$$

$$C^I_{KK+2} = C^I_{K+2K} = (1+\delta_{K0})^{1/2}[(I-K)(I+K+1)(I-K-1)(I+K+2)]^{1/2},$$

$$J_k(x_1,x_2) = J_k(\beta,\gamma) = 4B_k(\beta,\gamma)\beta^2\sin^2(\gamma - 2\pi k/3). \qquad (10)$$

The components Φ_{nIK} are subject to Neumann or Dirichlet boundary conditions at the boundary $\partial\Omega_2$ of the domain Ω_2 and the orhtogonality and normalization conditions

$$\int_0^{\beta_{\max}}\int_0^{\pi/3} g_0(\beta,\gamma)d\beta d\gamma \sum_{K\geq 0,even}^{I_{\max}} \Phi_{nIK}(\beta,\gamma)\Phi_{n'IK}(\beta,\gamma) = \delta_{nn'}. \qquad (11)$$

Exact solvable 5D harmonic oscillator (5DHO)

$$V(\beta,\gamma)=(C_2/2)\beta^2,\quad B_{\beta\beta}=B_{\gamma\gamma}=B_1=B_2=B_3=B_0,\quad B_{\beta\gamma}=B_{\gamma\beta}=0,$$

$$g_0(\beta,\gamma)=B_0 g_{11}(\beta,\gamma)=B_0\beta^2 g_{22}(\beta,\gamma)=B_0^{5/2}\beta^4\sin(3\gamma),\quad g_{12}(\beta,\gamma)=g_{21}(\beta,\gamma)=0.$$

Internal (a_0, a_2) and affine (b_0, b_2) coordinates

$$a_0=\beta\cos(\gamma)=b_0+\sqrt{\frac{2}{3}}b_2,\quad a_2=\frac{1}{\sqrt{2}}\beta\sin(\gamma)=b_2.$$

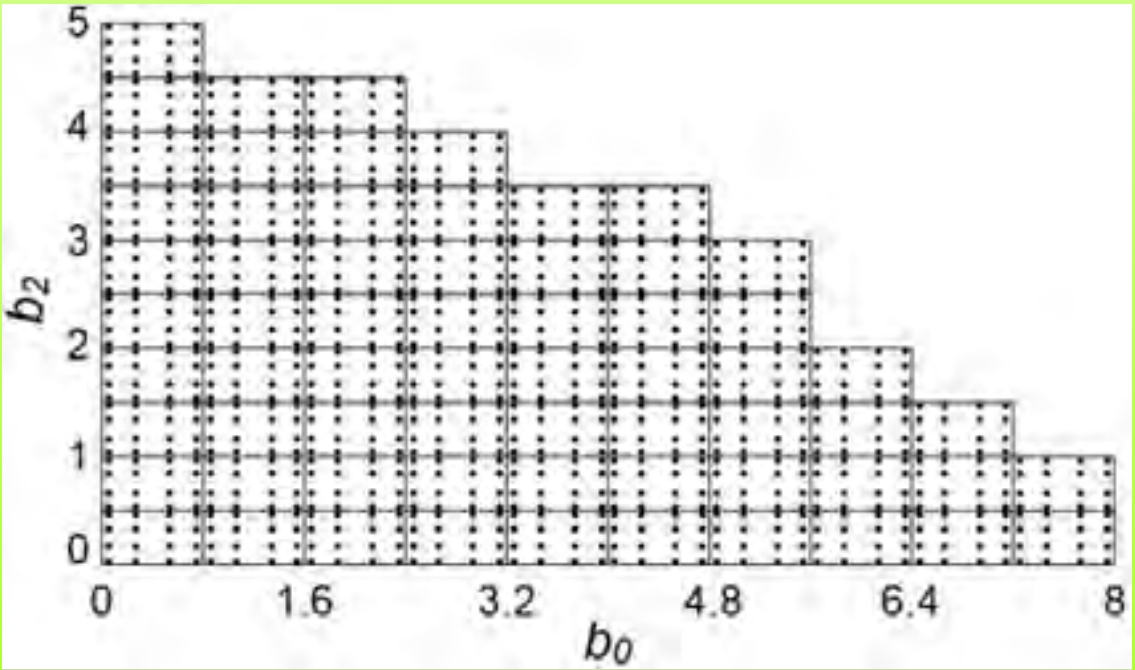

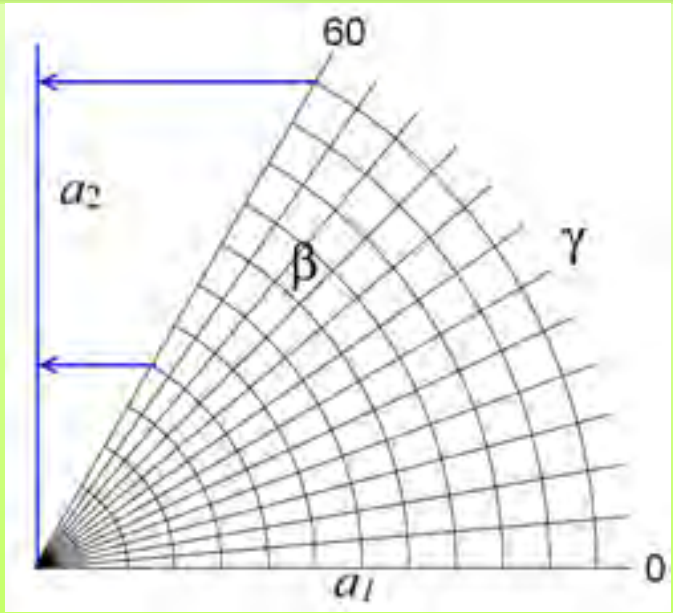

Rectangular grid of finite elements for the 5D harmonic oscillator. The Gaussian nodes are marked by circles.
In grid Ω_{b_0,b_2} the cells Δ_q for which $\min_{(b_0,b_2)\in\Delta_q} V(b_0,b_2) > 30$ are dropped.

Theoretical estimations of the order of the 2d FEM scheme

The Runge coefficients R_h were calculated in the grids $\Omega_{\beta,\gamma}$ and Ω_{b_0,b_2}

$$R_h = \log_2 \left| ((E_n^l)_h - (E_n^l)_{h/2})/((E_n^l)_{h/2} - (E_n^l)_{h/4}) \right|, \qquad (12)$$

where $(E_n^l)_h$, $(E_n^l)_{h/2}$, $(E_n^l)_{h/4}$ are the energies calculated by the program 2DFEM on the doubly condensed grids, gave estimates confirming the theoretical estimate of the order of $2p'$ of the 2d FEM scheme.

The discrepancies $\delta E_{l,n=1} = E^{\rm num}_{l,n=1} - E_{l,n=1}$ of the eigenvalues $E_{ln=1}$ of the 5DHO model in coordinates (β,γ) (left panel) and (b_0, b_2) (right panel) and Runge coefficients (12) (Ru) by the FEM schemes with LIPs and HIPs of the order p' =3.

l	h	$h/2$	$h/4$	Ru
0	5.4(-6)	9.2(- 8)	1.5(- 9)	5.88
2	9.6(-6)	1.6(- 7)	2.6(- 9)	5.92
3	1.4(-5)	4.2(- 7)	1.9(- 7)	5.93
0	1.4(-5)	2.8(- 7)	4.7(- 9)	5.62
2	2.2(-5)	4.7(- 7)	8.3(- 9)	5.57
3	2.9(-5)	1.2(- 6)	5.9(- 7)	5.47

l	h	$h/2$	$h/4$	Ru
0	3.1(-4)	8.0(-6)	1.3(- 7)	5.28
2	9.2(-4)	1.5(-5)	2.6(- 7)	5.92
3	2.8(-3)	4.4(-5)	7.6(- 7)	6.03
0	4.8(-4)	1.8(-5)	3.9(- 7)	4.68
2	1.2(-3)	3.3(-5)	7.4(- 7)	5.20
3	3.3(-3)	8.6(-5)	2.1(- 6)	5.27

The calculations are performed at $B_0 = 1$, $C_2 = 1$, and $\hbar = 1$ on the grids $\Omega_{\beta,\gamma} = [0(h_\beta)7] \otimes [0(h_\gamma)\pi/3]$ with $h_\beta = h, h/2, h/4$ at $h = 7/12$ and $h_\gamma = \pi/(36)$ and $\Omega_{b_0,b_2} = ([0(h_0)8] \otimes [0(h_2)5])$ with $h_0 = h, h/2, h/4$, $h_2 = 5h_0/8$ at $h = 8/7$.

Benchmark calculations of ^{154}Gd in the RMF model

Isolines of $V(\beta,\gamma)$ counted from the minimum of $V(\beta{=}0.3875,\gamma{=}0)$ $=-1270.6$MeV, $g_0(\beta,\gamma)$ and $g_{ij}(\beta,\gamma)$ of ^{154}Gd calculated in PC-F1 of RMF model

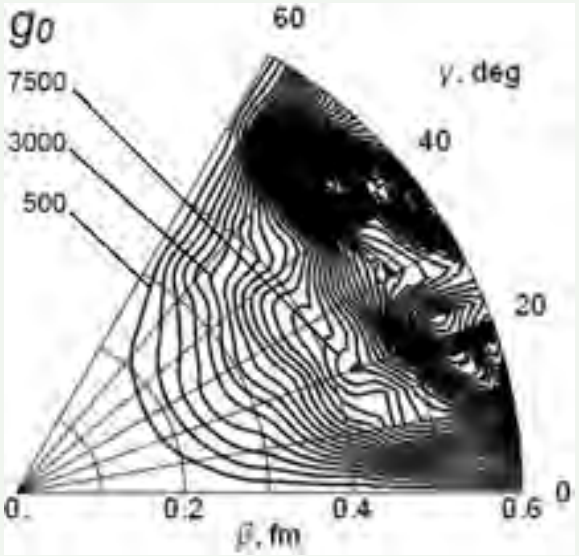

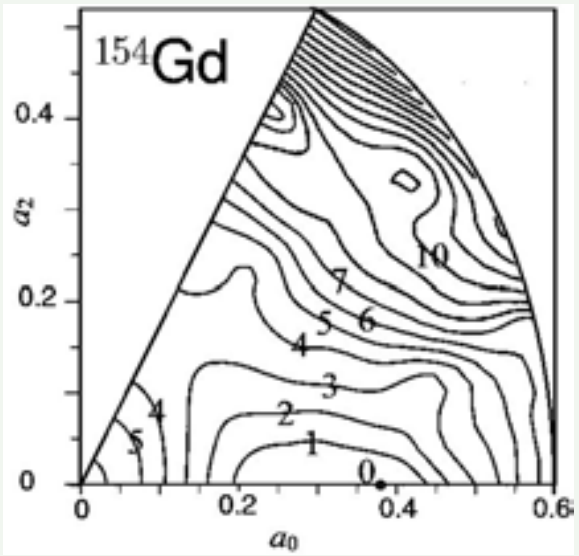

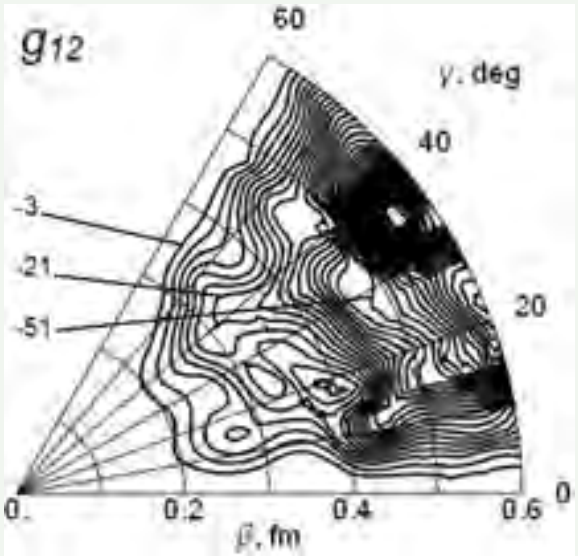

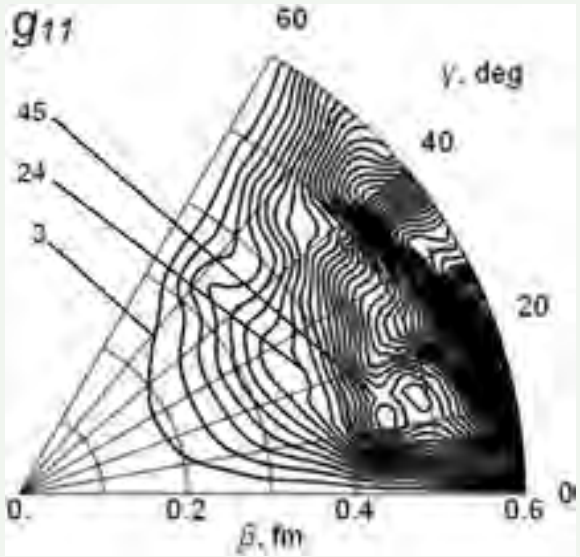

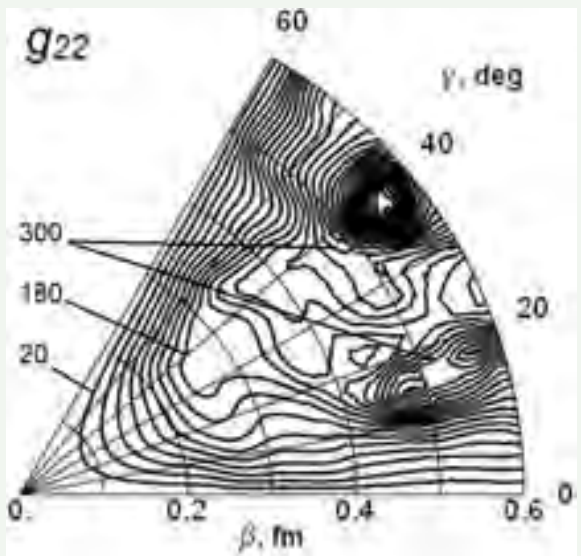

$$\hat{T}_{\rm vib}(\beta,\gamma) = -\frac{1}{g_0(\beta,\gamma)}\sum_{i,j=1}^{2}\frac{\partial}{\partial\beta}g_{ij}(\beta,\gamma)\frac{\partial}{\partial\gamma}.$$

Energy spectrum of ^{154}Gd and quasi-crossings of the energy bands

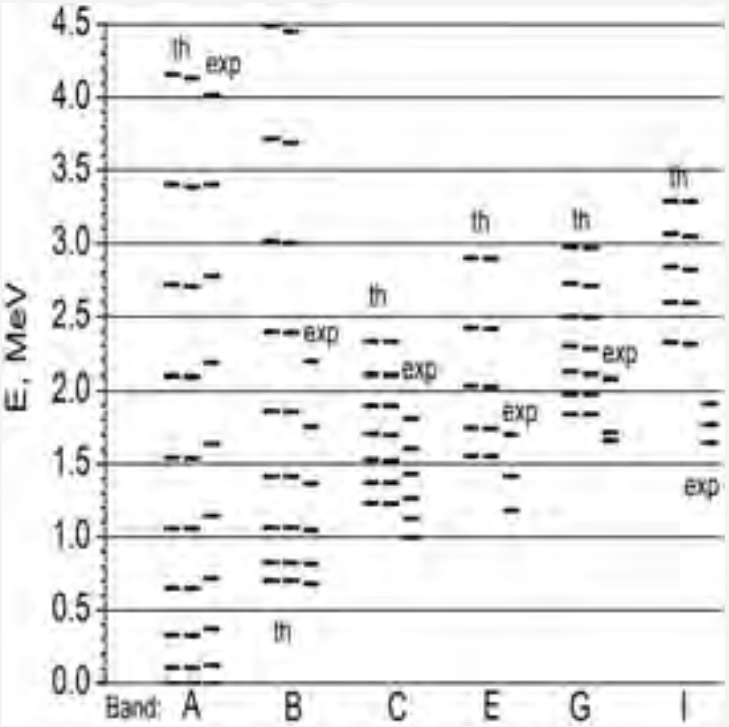

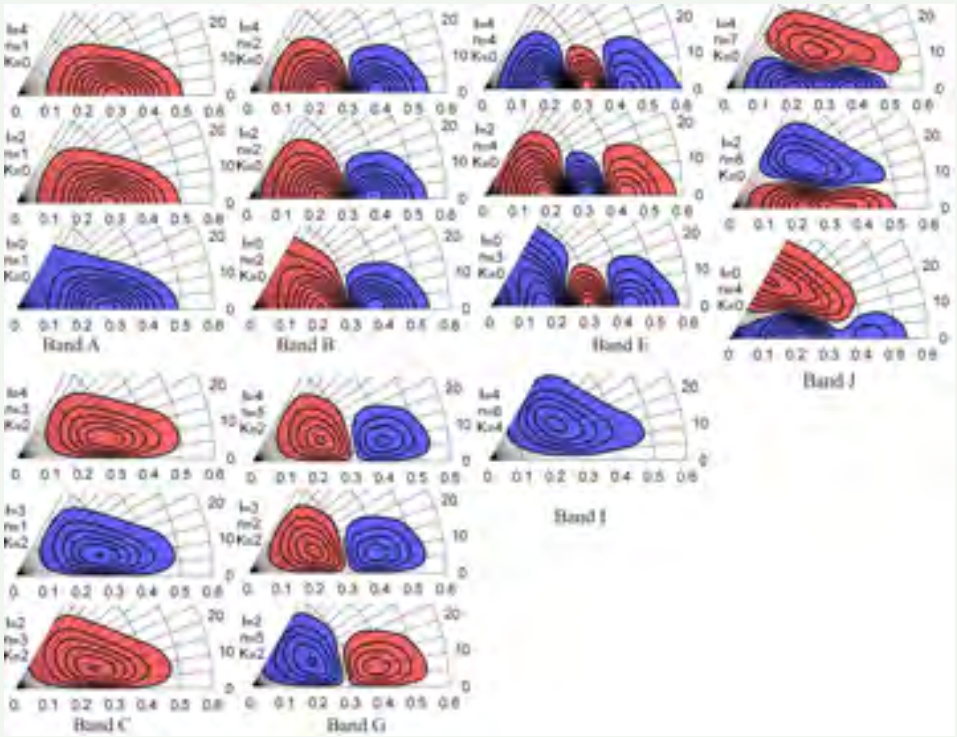

Energy spectrum of ^{154}Gd. For each state of the bands A, B, E, C, G, and I, three short bars correspond to the diagonal approximation (left), nondiagonal one (middle), and experiment (right)[http://www.nndc.bnl.gov/ensdf/].

Band(A) is the $K^\pi = 0+$ ground state band;
Band(B): the first excited $K^\pi = 0^+$ (β-vibrational) band;
Band(E), Band(J), Band(K): the second, third and forth excited $K^\pi = 0+$ bands;
Band(C): the $K^\pi = 2^+$ (γ-vibrational) band;
Band(G): the second excited $K^\pi = 2^+$ ($\beta\gamma$-vibrational) band;
Band(I): the $K^\pi = 4^+$ band.

Partial probability density integrals of components $\Phi_{nIK}(\beta,\gamma)$

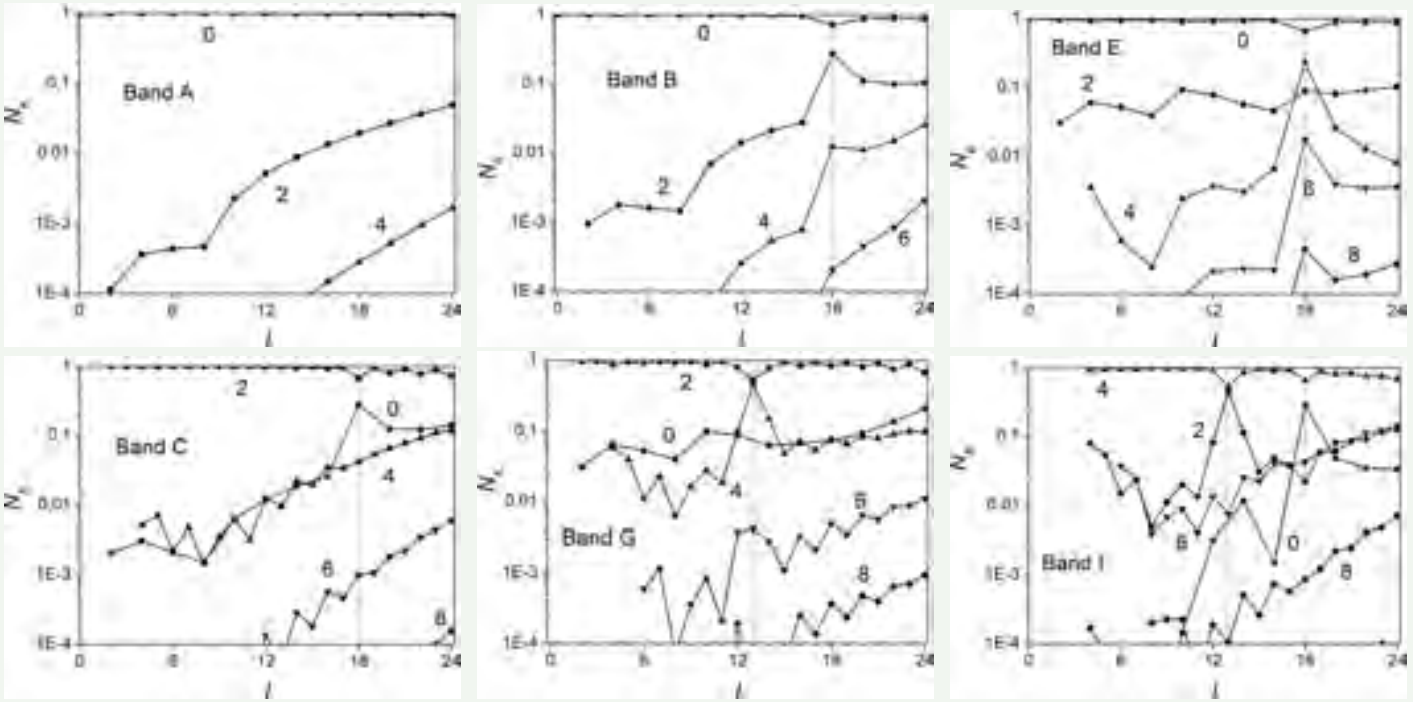

Integrals $N_K \equiv N^I_{Kn}$ from Eq. (13) for each of A, B, E, C, G, and I bands at the values of $K = 0, 2, 4, 6, 8$ labelling each of the curves.

$$N^I_{Kn} = \int_0^{\beta_{\max}} \int_0^{\pi/3} g_0(\beta,\gamma)\Phi_{nIK}(\beta,\gamma)\Phi_{nIK}(\beta,\gamma)d\beta d\gamma, \quad \sum_{K\geq 0,\text{even}}^{I} N^I_{Kn} = 1. \tag{13}$$

The leading values of diagonal approximation do also confirm the experimental classification of each of A, B, E, C, G, and I bands, while a selected agreement with the experimental data is due to the above restriction of the model parametrization.

Benchmark calculations of ^{154}Gd in the RMF model

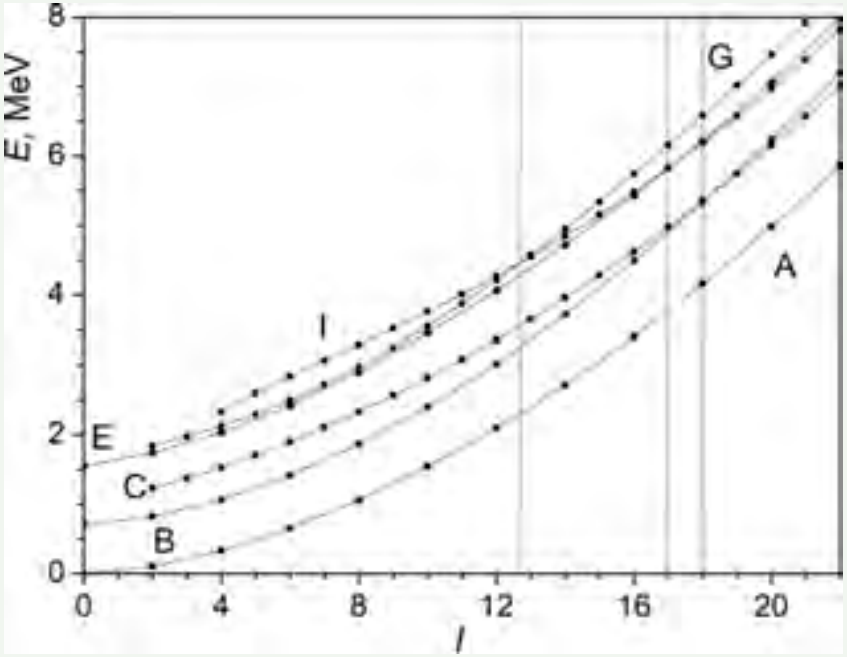

The lower part of the ^{154}Gd spectrum in the diagonal and nondiagonal approximation for each of A, B, E, C, G, and I bands used in the experimental data tables http://www.nndc.bnl.gov/ensdf/

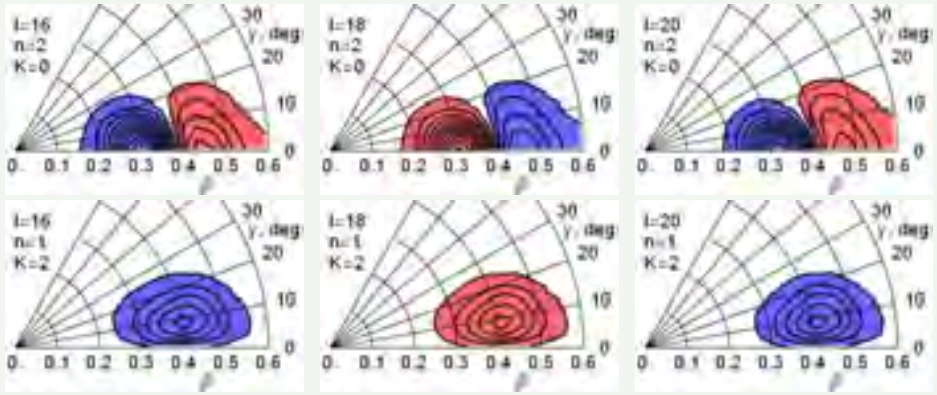

Isolines of the leading components $\Phi_{nlK} = \pm 0.01, \pm 0.03, \ldots$ of the ^{154}Gd wave functions for $n = 2, 3$ and $l = 16, 18, 20$ in diagonal approximation.

Benchmark calculations of ^{154}Gd in the RMF model

Band B

Band B

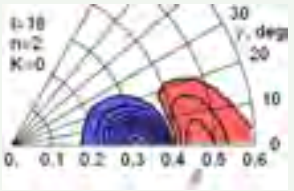

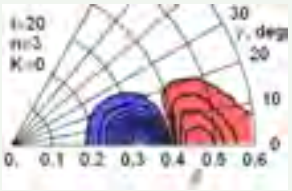

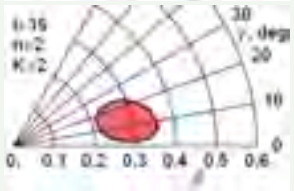

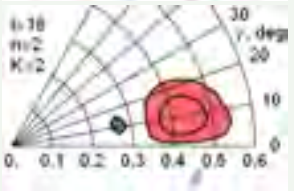

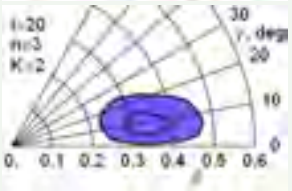

Band C

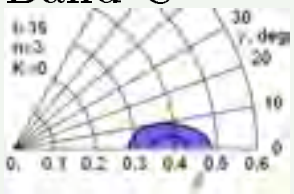

Band C

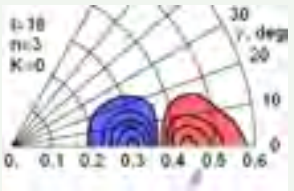

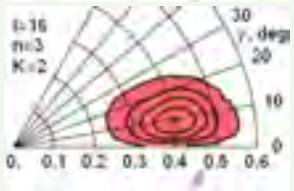

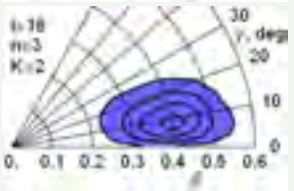

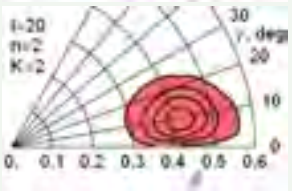

Isolines of the leading components $\Phi_{nlK} = \pm 0.01, \pm 0.03, \ldots$ of the ^{154}Gd wave functions for $n = 2, 3$ and $I = 16, 18, 20$ in nondiagonal approximations.

So, in the nondiagonal approximation at $I = 16$ and $I = 20$, the leading components practically coincide with those in the diagonal approximation, and at $I = 18$, the components are their linear combinations, belonging to both bands.

Calculated intraband and interband transitions

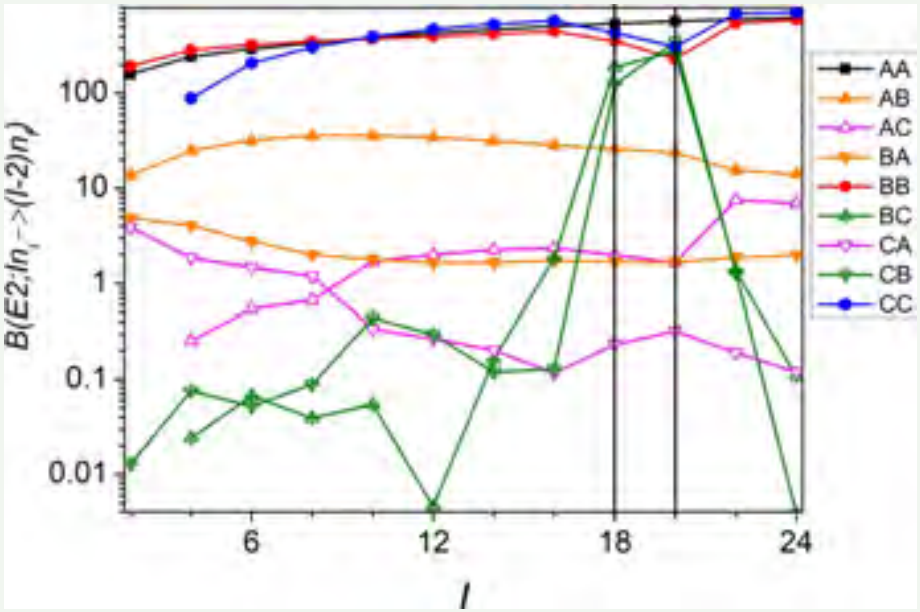

$B(E2)$	ndiag	diag	exp	bands
$2_1 \to 0_1$	160	159	157	AA
$4_1 \to 2_1$	244	243	245	
$6_1 \to 4_1$	294	293	285	
$8_1 \to 6_1$	341	339	312	
$10_1 \to 8_1$	387	385	360	
$2_2 \to 0_2$	194	193	97.0	BB
$0_2 \to 2_1$	68.5	69.2	52.0	BA
$2_2 \to 4_1$	45.0	45.5	19.6	
$2_3 \to 4_1$	0.460	0.248	1.72	CA
$2_3 \to 0_1$	3.89	4.14	5.70	

Calculated intraband and interband $B(E2; In_i \to (I-2)n_f)$ transitions between A, B and C bands in Weisskopf units (W.u.) in the nondiagonal approximation (nondiag) for ^{154}Gd.

In the vicinity of the quasi-crossing point at $I = 18$, the values of interband transitions between B and C bands are approximately 200 W.u., in comparison with small values (< 1 W.u.) beyond the vicinity.
However, the intraband transitions in the B and C bands in the vicinity of the quasi-crossing point are approximately by two times smaller than beyond the vicinity.

The potential energy surface and energy bands of ^{238}U in PC-PK1 RMF

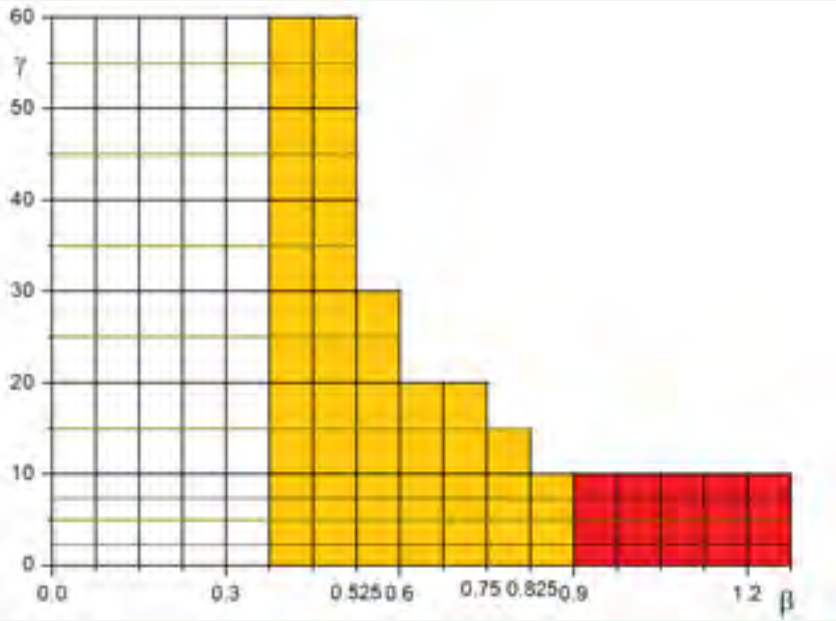

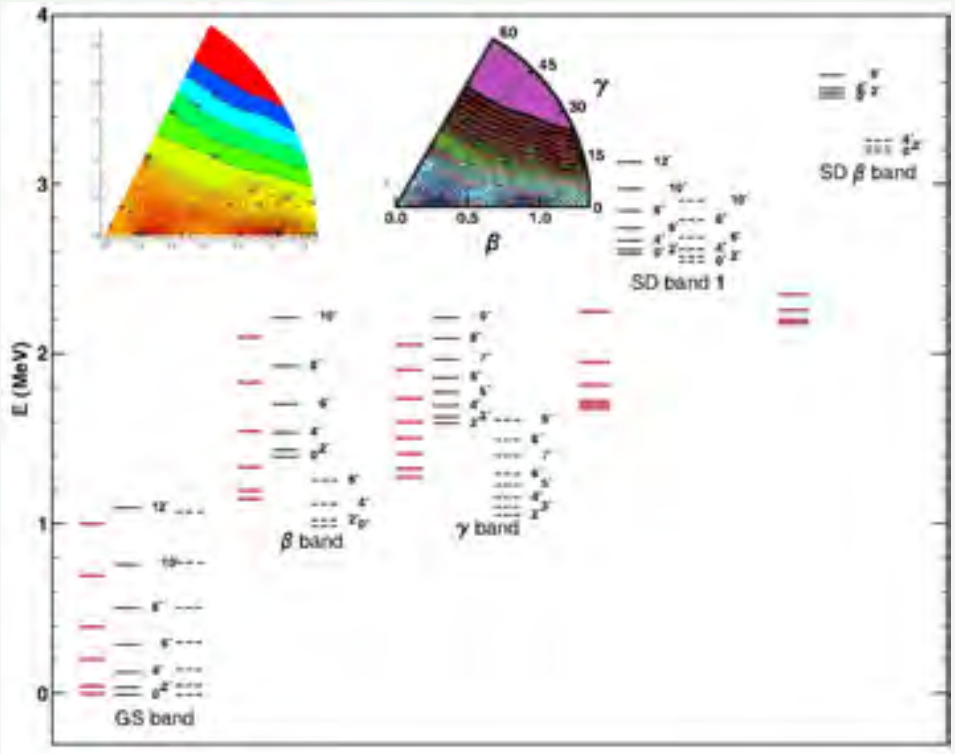

The 2d FEM grid and PES $V(\beta, \gamma)$ using in calculations by 2DFEM program of the $\pi = +$ energy levels E_{In} in the yrast and vibrational bands at normal and superdeformed shapes in ^{238}U marked by red bars;
Experimental and calculated values from [Libert, J., Girod, M. and Delaroche, J.-P.L.: Microscopic descriptions of superdeformed bands with the Gogny forces: Configuration mixing calculations in the A$\sim$190 mass region, Phys. Rev. C 60, 054301–1–26 (1999)] are shown as black dotted and solid bars. The insert is for $V(\beta, \gamma)$ in PC-PK1 RMF and in Gogny forces models.

The leading components of eigenfunctions of ^{238}U in PC-PK1 RMF

g.s.

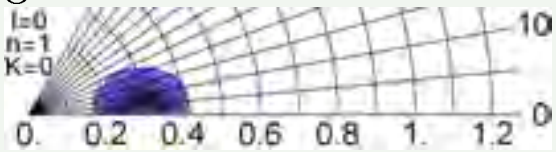

g.s.

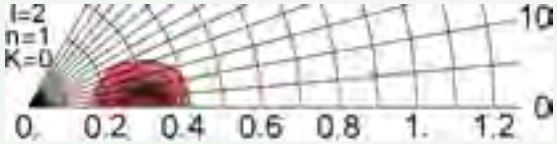

g.s.

γ

γ

β

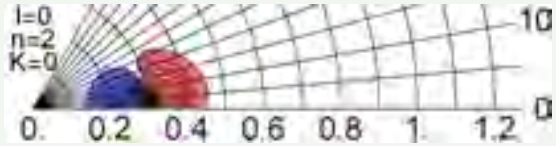

β

β

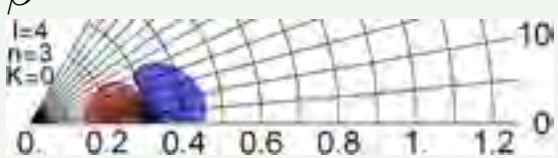

SD g.s.

SD g.s.

SD g.s.

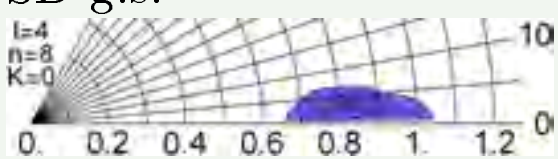

SD β

SD β

SD β

The leading components of eigenfunctions of ^{238}U in double well potential

Conclusion

• To solve elliptic multidimensional BVPs, the high-precision FEM schemes using Hermite interpolation polynomials on parallelepipeds are elaborated and applied to solve the BVP arising in the collective models of atomic nuclei.

• The efficiency of the algorithms and programs is demonstrated by benchmark calculations of the lower part of the quadrupole rotational-vibrational spectrum of the 5DHO model.

• The 2DFEM program benchmark calculations in PC-F1 or PC-PK1 parametrizations of the self-consistent RMF model of ^{154}Gd or ^{238}U isotopes are in an agreement with the single or double GTM basis sets calculations for single or double potential wells.

• The calculations of the quadrupole spectrum E_{In} of ^{154}Gd isotope and corresponding the reduced probabilities of electric interband and intraband $B(E2)$ transitions for the model based on RMF revealed a possibility of quasi-crossing of energy levels belonging to different bands at some values of the nucleus spin.

• The developed approach and 2DFEM programs provide a base for adapting multidimensional FEM programs to solving the bound state problems of the rotational-vibrational spectrum, which are applicable in generalizations of the geometric quadrupole collective model, the self-consistent relativistic mean-field (RMF) model and the quadrupole-octupole six-dimensional collective model of atomic nuclei.

Thank you for your attention!